


Article

Numerical Investigation on the Impact of Exergy Analysis and Structural Improvement in Power Plant Boiler through Co-Simulation

Hang Yin ^{1,2}, Yingai Jin ^{1,2,*}, Liang Li ³  and Wenbo Lv ^{1,2}¹ State Key Laboratory of Automotive Simulation and Control, Jilin University, Changchun 130022, China² College of Automotive Engineering, Jilin University, Changchun 130022, China³ Department of Engineering, School of Physics, Engineering and Computer Science, University of Hertfordshire, Hatfield AL10 9AB, Hertfordshire, UK

* Correspondence: jinya@jlu.edu.cn; Tel.: +86-431-85095196

Abstract: In current power station boilers, fuel burns at a low temperature, which results in low exergy efficiency. This research combined the second law of thermodynamics with the boiler structure to maximize the efficiency of a 350 MW power plant boiler. A three-dimensional simulation of the combustion process at the power plant boiler is performed. A one-dimensional simulation model of the boiler is then constructed to calculate the combustion exergy loss, heat transfer exergy loss, and boiler exergy efficiency. Under the principle of high-temperature air combustion technologies, this paper also proposes a new structure and improved operating parameters to improve the exergy efficiency of boilers by reducing the heat exchange area of the economizer and increasing the heat exchange area of the air preheater. Simulation results show that the exergy efficiency of the boiler increased from 47.29% to 48.35% through the modified model. The simulation outcomes can instruct future optimal boiler design and controls.

Keywords: power plant boiler; second law of thermodynamics; exergy efficiency; structural development



Citation: Yin, H.; Jin, Y.; Li, L.; Lv, W. Numerical Investigation on the Impact of Exergy Analysis and Structural Improvement in Power Plant Boiler through Co-Simulation. *Energies* **2022**, *15*, 8133. <https://doi.org/10.3390/en15218133>

Academic Editors: Yaojie Tu and Qingguo Peng

Received: 9 August 2022

Accepted: 28 October 2022

Published: 31 October 2022

Publisher's Note: MDPI stays neutral with regard to jurisdictional claims in published maps and institutional affiliations.



Copyright: © 2022 by the authors. Licensee MDPI, Basel, Switzerland. This article is an open access article distributed under the terms and conditions of the Creative Commons Attribution (CC BY) license (<https://creativecommons.org/licenses/by/4.0/>).

1. Introduction

Electricity is an indispensable portion of industrial production [1–3]. Renewable energy power generation technology faces technological dilemmas, such as unstable contribution to power generation, and therefore thermal power generation cannot be entirely replaced at the current stage [4–6]. Due to the lack of gas in China and its abundance of coal resources, coal remains the essential energy source [7–9]. At the same time, the proportion of coal-fired power generation in thermal power generation exceeds 90%, where coal is burned to provide electricity. One of the main devices in a power station is the boiler, which has been studied by a number of scholars.

During power generation boiler investigations, the energy analysis method is usually conducted to determine the energy loss distribution in the devices [10–14]. In order to achieve higher energy efficiency, using the concept of energy grade to analyze the irreversible loss in the operation process, rather than only focusing on the energy quantity, is also necessary, which is called the exergy analysis method [15–17]. Using the method, the work potential and energy efficiency of the system can be calculated [18–22]. Therefore, it is widely used in power system design and boiler improvement [23–27]. Shi [28] determined the boiler efficiency from soot blowing and proposed a superior model to improve the boiler performance. Francis Chinweuba et al. proposed that exergy analysis could be used to evaluate the performance of the system, including coal, biomass, and these raw materials as a combination of fuel [18]. The model can effectively identify the main parts of the damage and analyze the exergy losses of various parts. A new method of boiler exergy calculation for estimating the exergy loss and exergy efficiency was studied by

Behbahaninia et al. [23]. Gomez set up a model to simulate biomass boilers in a different environment and analyzed the results, which showed that an increase in oxygen concentration can reduce CO emissions [29]. In this study, the exergy loss of flue gas is divided into the physical component and the chemical component. The result showed that the primary source of exergy loss in the boiler accounted for a significant part of boiler energy loss. However, none of these studies addresses the distribution of energy loss and the optimization of the boiler structure. Furthermore, the current studies use a single software platform to analyze energy in the boiler. Due to the complex structure and boiler configurations, some conclusions from the original model may not apply.

In this paper, the proposed model is used to analyze the exergy loss of a 350 MW boiler in a power station and optimize the structure to minimize exergy loss during combustion. It is important to note that the critical point of the study introduced in this paper is the calculation of the exergy loss distribution using Aspen plus to redesign the boiler structure. The research contents of this article are as follows.

The physical model of the boiler based on boiler specifications is established with CFD.

Based on the second law of thermodynamics, the combustion model of the boiler furnace is developed under different load and coal conditions to observe the temperature field and flue gas distribution.

A one-dimensional combustion and heat transfer model is established with Aspen plus to simulate the heat transfer in superheater and reheater. The calculated value is then compared with the operation value to examine the accuracy. A MATLAB model is developed to calculate the exergy loss of heat transfer. The flow chart of the study is shown in Figure 1.

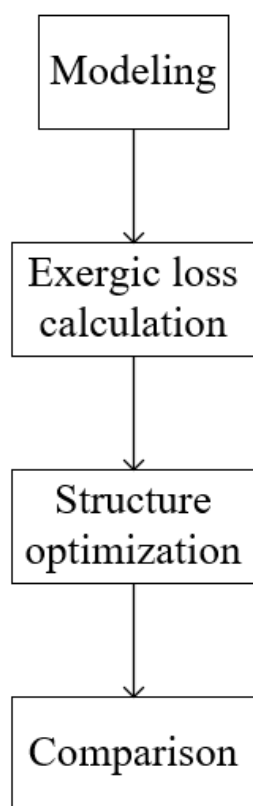


Figure 1. Flow chart.

A structural modification scheme is formulated in order to minimize exergy loss. The heat transfer capacity of the economizer decreases, and the heat transfer capacity of the air preheater increases in this scheme. As a result, the burning exergy loss of the boiler was

reduced. The exergy loss of heat transfer was reduced, and the exergy efficiency of the boiler was improved by improving the steam parameters.

2. System Parameters and Exergy Analysis Mathematical Model

The 350 MW boiler is a supercritical boiler in a power plant in Changchun, China and its design parameters are formulated in Table 1 and the coal type parameters are shown in Table 2.

Table 1. Main parameters of boiler.

Parameter	Unit	Boiler Maximum Continuous Rating (BMCR)	75%BMCR	50%BMCR
Superheated steam flow of the boiler	t/h	1110	723.72	555
Superheater outlet steam pressure	MPa(g)	25.40	19.73	14.49
Superheater outlet steam temperature	°C	571	571	571
Reheat steam flow	t/h	929.17	623.45	484.70
Reheater inlet steam pressure	MPa(g)	4.524	3.014	2.296
Reheater outlet steam pressure	MPa(g)	4.334	2.885	2.194
Reheater inlet steam temperature	°C	323	311.6	321.5
Reheater outlet steam temperature	°C	569	569	569
Economizer inlet feed water temperature	°C	284.7	258.9	244.3

Table 2. Design coal parameters.

Parameter	Notation	Unit	Design Coal
Total moisture	Mar	%	27.8
Air dry base moisture	Mad	%	9.27
Receive base ash	Aar	%	12.06
Dry ash-free volatiles	Vdaf	%	45.09
Received base carbon	Car	%	47
Received base hydrogen	Har	%	3.50
Received base oxygen	Oar	%	8.85
Received base nitrogen	Nar	%	0.60
Received base sulfur	Sar	%	0.19
Low heat value	Qnet.ar	MJ/kg	17.34

Coal type parameters are shown in Table 2.

2.1. Exergy Efficiency

Exergy efficiency is an index based on the second law of thermodynamics to measure the energy conversion and thermodynamic perfection of the thermodynamic systems. The definition expression of exergy efficiency is as follows [30]:

$$\eta = \frac{A_{x,g}}{A_{x,n}} = 1 - \frac{A_{x,L}}{A_{x,n}} \quad (1)$$

where $A_{x,g}$ is the income exergy, $A_{x,L}$ is the exergy loss, and $A_{x,n}$ is the total input exergy.

2.2. Fuel Exergy Calculation

$$a_B = LHV(1.0064 + 0.1519\frac{H}{C} + 0.0616\frac{O}{C} + 0.0429\frac{N}{C}) \quad (2)$$

where LHV is the low calorific value; $C, H, O, N,$ and S represent the mass fractions of carbon, hydrogen, oxygen, nitrogen, and sulfur in the fuel, respectively. The Xinze formula of solid fuel is used to calculate the fuel from coal in this analysis.

2.3. Calculation of the Boiler External Loss

The boiler external loss can be calculated according to the thermal efficiency of the boiler. The exergy loss of the exhaust gas is calculated with its temperature.

$$a_2 = V_y c_p (T_{py} - T_0 - T_0 \ln \frac{T_{py}}{T_0}) \quad (3)$$

where V_y is the volume of the flue gas, T_0 is the temperature of the environment, c_p is the average constant pressure specific heat of the flue gas, and T_{py} is the exhaust temperature, which is 147 °C under BMCR load.

As shown in the following formulae, the exergy loss associated with the incomplete combustion of gases and solids is calculated:

$$a_3 = a_B q_3 \quad (4)$$

$$a_4 = a_B q_4 \quad (5)$$

in which a_B is the fuel exergy, q_3 is the heat loss of the incomplete combustion of the combustible gas, and q_4 is the heat loss of the incomplete combustion of the solid.

$$q_{5,ed} = 5.82(D_{ed})^{-0.38} \quad (6)$$

$$Q_5 = q_{5,ed} \frac{D_{ed}}{D} \quad (7)$$

in which D_{ed} is the rated evaporation capacity, $q_{5,ed}$ is the heat loss at rated evaporation, D is the actual evaporation, Q_5 is heat dissipation loss under non-rated operating conditions, and $q_{5,ed}$ is the heat dissipation loss of the boiler at the rated evaporation volume.

The heat exergy loss can be determined by the following equation:

$$a_5 = Q_5 (1 - \frac{T_0}{T_B}) \quad (8)$$

where T_B is the average temperature of the working fluid in the heat dissipation part of the boiler. In this project, 400 °C was selected for the simplicity of the calculation process.

The exergy loss of ash was determined by the following equation.

$$a_6 = \frac{A_y}{100} \left[\frac{\alpha_{lz}(t_{lz} - t_0)c_{lz}}{100 - c_{lz}^c} (1 - \frac{T_0}{T_{lz}}) + \frac{\alpha_{fh}(\theta_{py} - t_0)c_{fh}^c}{100 - c_{fh}^c} (1 - \frac{T_0}{T_{py}}) \right] \quad (9)$$

where A_y is the applied base ash; t_{lz} is the slag temperature discharged from the furnace, °C; θ_{py} is the exhaust gas temperature, °C; c_{lz}^c and c_{fh}^c are the content of slag and fly ash, %; and c_{lz} and c_{fh} are the specific heat of slag and fly ash, which can be found in the table, kJ/kg. The external exergy loss is the sum of these losses.

2.4. Calculation of the Combustion Exergy Loss in Boiler

According to the national standard GB/T140909-2005 Energy System Exergy Analysis Technical Guidelines, the expression for the exergy loss of combustion is shown below:

$$I_r = M_f a_B - M_f V_g \int_{T_0}^{T_h} C_p (1 - \frac{T_0}{T}) dT \quad (10)$$

where M_f is the amount of fuel, kg/h; V_g is the volume of flue gas produced per kilogram of fuel, m^3/kg ; C_p is the average constant pressure specific heat of the flue gas, $\text{kJ}/(\text{m}^3 \cdot \text{K})$; and T_h is the maximum temperature of the flue gas when the boiler burns.

2.5. Calculation of Boiler Heat Transfer Exergy Loss

The formula for heat transfer exergy loss is shown below:

$$A_c = \delta Q T_0 \left(\frac{1}{\bar{T}_c} - \frac{1}{\bar{T}_h} \right) \quad (11)$$

where δQ is the unit heat transfer, kJ/kg ; T_0 is the ambient temperature, K; \bar{T}_c is the average temperature of the cold fluid, K; \bar{T}_h is the average temperature of the hot fluid, K.

$$\bar{T}_c = (T_{c1} - T_{c2}) / \ln \frac{T_{c1}}{T_{c2}} \quad (12)$$

$$\bar{T}_h = (T_{h1} - T_{h2}) / \ln \frac{T_{h1}}{T_{h2}} \quad (13)$$

where T_{c1} is the inlet temperature of the cold fluid, K; T_{c2} is the outlet temperature of the cold fluid, K; T_{h1} is the inlet temperature of the hot fluid, K; and T_{h2} is the outlet temperature of the hot fluid, K.

The exergy loss of each heat exchanger in the tail flue can be calculated according to the exergy analysis and calculation formula mentioned. The exergy loss of the heat transfer was programmed in Matlab to calculate the heat transfer. On the basis of Power Station Course Design Instructions, the boiler combustion calculation formula is established. The exergy loss of each heat exchanger in the boiler flue was calculated. The exergy loss distribution of each part can be clearly analyzed by this procedure. The flow of the program is shown in Figure 2.

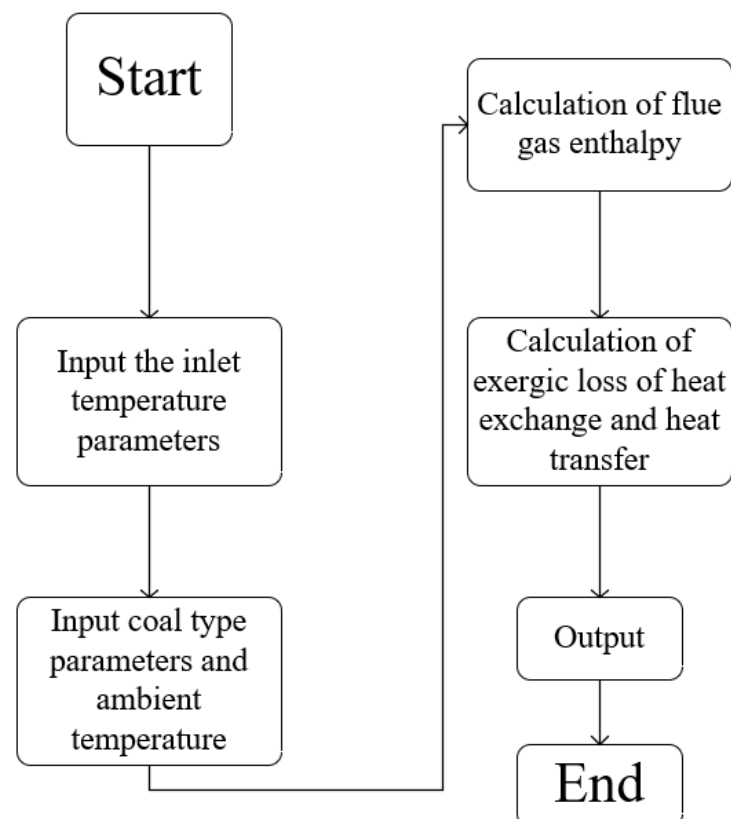


Figure 2. Flow of the program.

2.6. Physical/Chemical Model

2.6.1. Gas Turbulence Equation

The realizable turbulence model was adopted in this simulation. The term “realize” means to ensure that there are mathematical constraints in Reynolds pressure, so as to ensure the continuity of turbulence. The equation is as follows:

$$\frac{\partial(\rho k)}{\partial t} + \frac{\partial(\rho k u_i)}{\partial x_i} = \frac{\partial}{\partial x_i} \left[\left(\mu + \frac{\mu_i}{\sigma_k} \right) \frac{\partial k}{\partial x_i} \right] + G_k + G_b - \rho \varepsilon - Y_M + S_k \quad (14)$$

$$\frac{\partial}{\partial \tau} (\rho \varepsilon) + \frac{\partial}{\partial x_i} (\rho \varepsilon u_i) = \frac{\partial}{\partial x_i} \left[\left(\mu + \frac{\mu_\varepsilon}{\sigma_\varepsilon} \right) \frac{\partial \varepsilon}{\partial x_i} \right] + \rho C_1 E \varepsilon - C_2 \rho \frac{\varepsilon^2}{k + \sqrt{\nu \varepsilon}} \quad (15)$$

where $\sigma_\varepsilon = 1.2$, $C_1 = \max \left[0.43, \frac{\eta}{\eta+5} \right]$, $C_2 = 1.9$, $\eta = (2E_{ij}E_{ji})^{1/2} \frac{k}{\varepsilon}$, $E_{ij} = \frac{\partial \mu_i}{\partial x_j} + \frac{\partial \mu_j}{\partial x_i}$.

2.6.2. Gas Solid Two-Phase Flow Equation

Pulverized coal combustion belongs to the gas–solid two-phase flow. The Lagrangian stochastic particle trajectory model is adopted, which is more consistent with the actual situation in the furnace and is suitable for volatilization and heterogeneous reactions. The force equation of particles is as follows:

$$\frac{du_p}{dt} = F_D(u - u_p) + g \frac{(\rho_p - \rho)}{\rho_p} + F \quad (16)$$

where u is the fluid phase velocity, m/s; $u - u_p$ is the difference between fluid phase velocity and particle velocity, m/s; $F_D(u - u_p)$ is the force on particles per unit of mass; ρ_p is the density of particles, kg/m³; and $g \frac{(\rho_p - \rho)}{\rho_p}$ represents the buoyancy force on the particle.

2.6.3. Pulverized Coal Combustion Model

The pulverized coal combustion model can be divided into three models, which are volatilization analysis, gas phase combustion, and coke burning models. The equations of these three models together constitute the pulverized coal combustion model.

The volatilization analysis model of pulverized coal is a two-path model, as follows:



M_0 represents pulverized coal and M_1 represents coke. The first equation is preferred for low-temperature reactions, and the second equation is chosen for high-temperature reactions.

The gas-phase combustion model is applied to the non-premixed simulation method. If the simulation includes small droplets or coal particles, the non-premixed model is applied. The formula is:

$$f = \frac{Z_i - Z_{i,ox}}{Z_{i,fuel} - Z_{i,ox}} \quad (19)$$

where Z_i refers to the mass fraction of the element; $Z_{i,ox}$ refers to the content at the inlet of the oxidant; and $Z_{i,fuel}$ refers to the value at the inlet of the fuel.

The reaction rate of coke combustion is:

$$D_0 = C_1 \frac{[(T_p + T_\infty)/2]^{0.75}}{d_p} \quad (20)$$

where T_∞ is the ambient temperature, K; C_1 is the diffusion rate constant; T_p is the temperature of the particle; and d_p is the average particle diameter of coke, m.

2.6.4. Radiation Model

The P-1 radiation heat transfer model is adopted in this study. This model not only considers the scattering effect of radiation, which is suitable for the actual situation of the boiler, but is also a relatively simple model, which greatly reduces the calculation time, so this model is preferred.

$$q_r = -\frac{1}{3(\alpha + \sigma_s) - C\sigma_s} \nabla G \quad (21)$$

where σ_s is the diffusion coefficient, α is the absorption coefficient, G is the amount of incident radiation, and C is the coefficient of the linear anisotropic phase function. When using this model, strict attention should be paid to the optical thickness. In order to obtain the best convergence effect, the optical thickness $(\alpha + \sigma_s)L$ must be 0.01–10.

2.6.5. Model of Coupling of Velocity and Pressure

In the solver setting, the coupling model of pressure and velocity is formulated in the form of the Navier–Stokes equation:

$$\begin{cases} \rho \left(\frac{\partial \mathbf{u}}{\partial t} + \mathbf{u} \cdot \nabla \mathbf{u} \right) = \rho \mathbf{f} - \nabla p + \mu \nabla^2 \mathbf{u} \\ \mathbf{u}(\mathbf{x}) = \mathbf{u}_b \mathbf{x} \in \partial V_1 \\ \mathbf{n} \cdot \mathbf{u}(\mathbf{x}) = 0, \mu \frac{\partial \mathbf{u}_t(\mathbf{x})}{\partial \mathbf{n}} = -\beta p \mathbf{u}, \mathbf{x} \in \partial V_2 \end{cases}$$

where p is the macroscopic pressure and \mathbf{u} is the velocity.

3. Description of the Model

The boiler in this paper is a 350 MW supercritical boiler from a power plant in Changchun, which is a single-furnace boiler with single intermediate reheating. The designed coal is lignite. The main structure size is 14.6 m × 58.3 m (length × height), and the aspect ratio is 1.

In this study, FLUENT was first used to simulate the distribution of exergy, and then Aspen Plus was used to calculate the temperature of each part of the boiler. Finally, heat transfer exergy was calculated in MATLAB.

3.1. Model of the Boiler Furnace

CATIA software was used to make a general assembly 3D model, and the analysis of the coal combustion process was carried out using FLUENT. Different grids were set up in each region by ICEM software. As a result, combustion characteristics and temperature distributions could be accurately determined. There were four main areas in ICEM for the boiler mesh. As shown in Figure 1a, the lowest part is the dry bottom hopper area, where the grid does not need to be encrypted, followed by the main burner area, the separate over-fire air (SOFA) area, and the horizontal flue and flare Angle area. As shown in Figure 3, the mesh with maximum density is located in the SOFA burner area. The horizontal flue and furnace arch are located at the top of the boiler. The inlet boundary conditions are shown in Table 3.

In this paper, the temperature difference between the inlet and outlet was used as the test index, that is, the temperature difference of the simulation will not change with the increase in the number of grids. At this time, the number of grids can ensure the accuracy of the simulation on the one hand, and the simulation time will not be too long on the other hand. The variation of temperature differences with the number of grids is shown in Table 4.

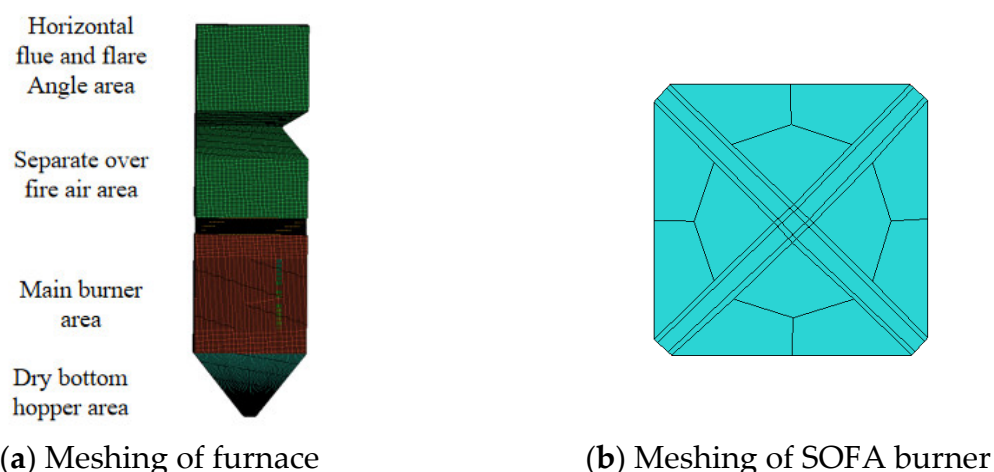


Figure 3. Mesh generation of the furnace (a) and SOFA burner (b).

Table 3. The temperature difference varies with the grid numbers.

Name	Unit	Number
Primary air temperature	K	338
Secondary air temperature	K	653
Burnout air temperature	K	653
Primary wind velocity	m/s	25
Secondary air velocity	m/s	48
Burnout wind velocity	m/s	48
Pulverized coal fineness (R90)	%	37
Pulverized coal mass flow rate	kg/s	2.542

Table 4. The variation of temperature difference with the grid numbers.

N	Number of Grids	Temperature Difference(K)	Error
1	1,862,248	0.842	-
2	2,421,385	0.910	2.4%
3	3,342,675	0.931	3.2%
4	4,769,510	0.934	0.5%
5	6,102,687	0.935	0.2%

3.2. Comparison Analysis of Flue Gas in the Furnace under Different Load Conditions

In this study, we use the Realizable turbulence model. Regarding the combustion process, the model adopted in the study is a non-premixed combustion model, which is often used in boiler simulation. The simulation process is carried out after the coal type parameter is input.

The distribution of smoke and gas in the furnace under different loads is shown in Figure 4. Figure 4a–c show that the maximum value of flue gas decreases as the load is reduced. The overall flue gas distribution has a certain regularity despite subtle differences, which is explained by the component distribution. Figure 4d shows that the flue gas exergy also rises with height. In the burner, flue gas has a higher value. In addition, flue gas exergy peaks at the same position under different loads, which indicates that this region still has the potential to reduce loss before reaching the peak value. Combustion exergy loss could be reduced by increasing the air temperature at the inlet when the air enters the furnace.

3.3. Power Plant Boiler Model Construction

This article presents a boiler model built by Aspen Plus using the RYield module, the RGibbs module, and the SSplit module. RYIELD is suitable for reactions in which the reaction relationship is unknown, the reaction kinetic parameters are unknown, but the

product distribution ratio is known. The flow rates of various products can be calculated by inputting product yields or Fortran subroutines. RGibbs is a reactor that simulates single-phase chemical equilibria, phase equilibria without chemical reactions, and multiple components simultaneously in phase and chemical equilibria using the Gibbs free energy minimization principle. The HeatX module simulates the heat exchange between the two logistics. The heatx model determines the state of the export logistics according to the conservation of energy and mass. As shown in Figure 5, the RYield module is used to pyrolyse coal. RGibbs represents the Gibbs reaction. The heat flow Q-DECOMP generated during the pyrolysis process is connected to the RGibbs module to ensure the balance of heat in the system. Q-LOST determines the heat dissipation of the boiler and excludes it. The SSplit module separates the flue gas and ash, allowing the ash to be discharged and the flue gas to continue exchanging heat.

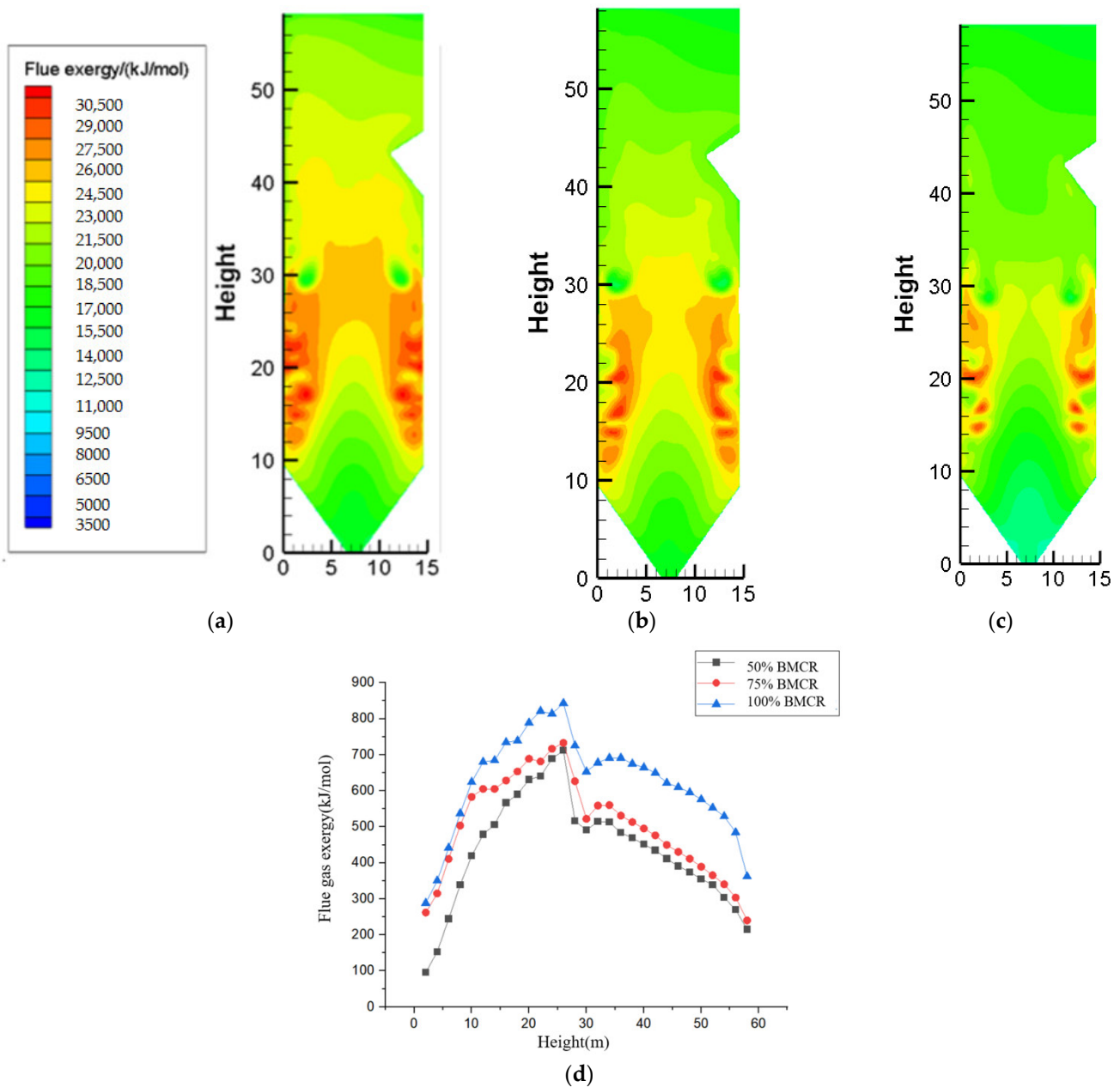


Figure 4. Distribution of flue exergy and flue gas exergy under different loads. (a) 100%BMCR. (b) 75%BMCR. (c) 50%BMCR. (d) Distribution of flue gas on the height of the furnace.

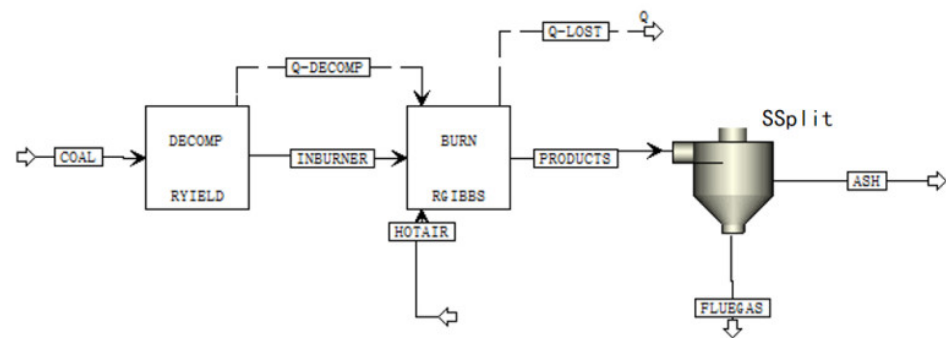


Figure 5. Combustion system module.

As shown in Figure 6, the HeatX module is used to carry out the design calculation according to the boiler design manual. The flue gas is divided into two streams, among which one flows through the low-temperature reheater (L-RH), and the other flows through the low-temperature superheater (L-SH) and the economizer (ECONOM). Then the two streams pass through the air preheater (PHAIR) and merge into the air. Before they can be discharged into the environment, these exhaust gases must be dedusted and reduced.

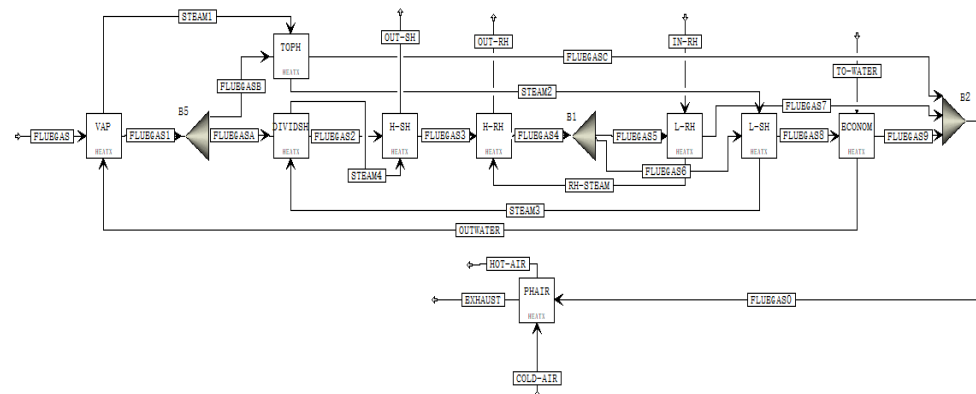


Figure 6. Heat exchange system module.

The feed water (TO-WATER) is heated by the economizer and turned into hot water (OUTWATER). Meanwhile, the heat exchange temperature in the water-cooled wall increases. Afterwards, it is heated by a roof superheater (TOPH), low-temperature superheater, partition screen superheater, and high-temperature superheater and turned into superheated steam. In the final step, superheated steam is transferred to a steam turbine. The reheated steam (IN-RH) is heated by a low-temperature reheater and a high-temperature reheater and supplied to the steam turbine. The airflow is cold air (COLD-AIR) in the air preheater, and heat is exchanged with the tail flue gas and turned into hot air (HOT-AIR). Combustion and heat transfer system flow charts are combined to form a closed cycle, which constitutes the entire system of the boiler. That is, the flue gas separated from the SSplit module passes through the water wall, and the hot air from the air preheater participates in the combustion. The overall model diagram is shown in Figure 7.

3.4. Model Input Parameter Settings

There are some input parameters for the module, which are shown in Table 5.

3.5. Model Simulation Results

As shown in Tables 6 and 7, the accuracy of the model can be verified based on the simulation results and the operation data provided by the power plant. The full names of BMCR, DIVIDSH, H-SH, H-RH, L-RH, L-SH, and ECONOM are shown in the nomenclature at the end of the article.

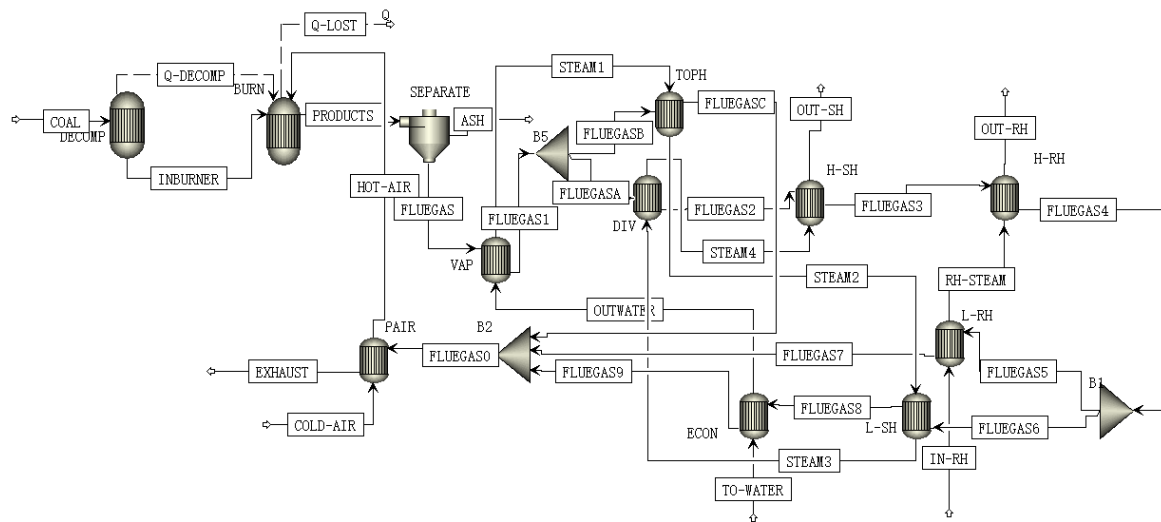


Figure 7. General diagram of boiler system model.

Table 5. Input parameter settings of model.

Environment	Temperature 25 °C. Pressure 101,325 Pa
Air	Under BMCR condition, oxygen 289,686 kg/h, nitrogen 1,089,769 kg/h
To-water	Temperature 284.7 °C, pressure 28.87 MPa, flow 1,110,000 kg/h
Main steam	Temperature 571 °C, pressure 25.40 MPa, flow 1,110,000 kg/h
Reheat steam inlet	Temperature 323 °C, pressure 4.524 MPa, flow 929,170 kg/h
Reheat steam outlet	Temperature 569 °C, Pressure 4.334 MPa
Amount of fuel	183,040 kg/h
M_{ar}	27.8%
M_{ad}	9.27%
A_{ar}	12.06%
V_{daf}	45.09%
C_{ar}	47%
H_{ar}	3.5%
O_{ar}	8.85%
N_{ar}	0.60%
S_{ar}	0.19%

Table 6. Comparison table of working fluid simulation calculation results.

Parameter	BMCR		75%BMCR		50%BMCR	
	Simulation Results (°C)	Operation Results (°C)	Simulation Results (°C)	Operation Results (°C)	Simulation Results (°C)	Operation Results (°C)
Inlet of DIVIDSH	466	482	442	465	425	442
Outlet of DIVIDSH	526	540	512	538	505	529
Inlet of H-SH	526	540	512	538	505	529
Outlet of H-SH	571	571	571	571	571	571
Inlet of H-RH	473	472	461.6	477	461.5	481
Outlet of H-RH	569	569	569	569	557.5	545.8
Inlet of L-RH	323	323	311.6	311.6	321.5	321.5
Outlet of L-RH	473	472	461.6	477	461.5	481
Inlet of L-SH	418	428	394	408	377	380
Outlet of L-SH	466	482	442	465	425	442
Inlet of ECONOM	284.7	284.7	258.9	258.9	244.3	244.3
Outlet of ECONOM	309	307	284	280	269	267

Table 7. Comparison table of flue gas simulation calculation results.

Parameter	BMCR		75%BMCR		50%BMCR	
	Simulation Results (°C)	Operation Results (°C)	Simulation Results (°C)	Operation Results (°C)	Simulation Results (°C)	Operation Results (°C)
Inlet of DIVIDSH	1201	1210	1103	1100	997	1002
Outlet of DIVIDSH	1068	1069	975	973	873	918
Inlet of H-SH	1068	1069	975	973	873	918
Outlet of H-SH	977	986	878	894	778	842
Inlet of H-RH	977	971	878	879	778	827
Outlet of H-RH	864	859	759	781	676	737
Inlet of L-RH	864	821	759	742	676	697
Outlet of L-RH	415	387	390	373	384	374
Inlet of L-SH	864	821	759	742	676	697
Outlet of L-SH	568	560	530	510	505	475
Inlet of ECONOM	568	560	530	510	505	475
Outlet of ECONOM	415	442	390	389	384	358

The accuracy of the model is demonstrated by comparing the calculated and plant values of BMCR, 75% BMCR, and 50% BMCR loads. Consequently, the model can be used to calculate other boiler load conditions, and the calculation method is similar to how the boiler operates.

4. Exergy Analysis Calculation Result Comparison

Matlab software is used to calculate heat transfer exergy loss according to the exergy analysis method mentioned above, and then the heat transfer exergy loss of each heat exchanger under different loads is calculated, as depicted in Tables 8–10.

The overall exergy efficiency of the boiler is shown in Figure 8. As the load decreases, the exergy efficiency decreases gradually, and the overall exergy loss increases. Hence, it is necessary to avoid reducing the load to use energy effectively.

The heat transfer exergy losses under various loads are depicted in Figure 9. There is almost no difference in the distribution of heat transfer exergy losses by the different loads. WALL and L-RH have significant heat transfer exergy losses. One of them only flows through the low-temperature reheater, while the other flows through the L-RH and the economizer, resulting in a large heat transfer difference in the L-RH. It is possible to reduce exergy loss by improving the arrangement of heating surfaces in these two positions.

Table 8. Distribution of heat transfer exergy loss of boiler under BMCR load.

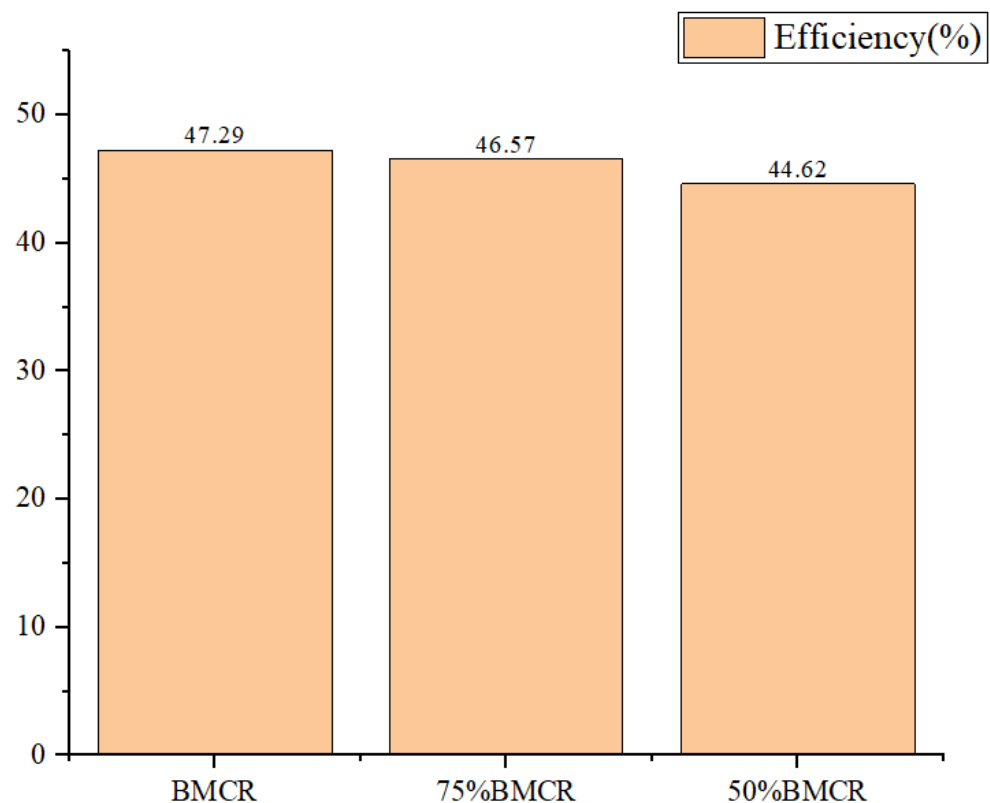
Parameter	Notation	Unit	Percentage of Fuel Exergy (%)
Total	3667.52	kJ/kg standard coal	20.53
Water wall and roof superheater	1222.07	kJ/kg standard coal	6.84
Platen superheater	319.54	kJ/kg standard coal	1.79
High temperature superheater	162.67	kJ/kg standard coal	0.91
High temperature reheater	189.09	kJ/kg standard coal	1.06
Low temperature reheater	646.95	kJ/kg standard coal	3.62
Low temperature superheater	433.95	kJ/kg standard coal	2.43
Economizer	253.14	kJ/kg standard coal	1.42
Air preheater	440.11	kJ/kg standard coal	2.46

Table 9. Distribution of heat transfer exergy loss of boiler under 75% BMCR load.

Parameter	Notation	Unit	Percentage of Fuel Exergy (%)
Total	3602.38	kJ/kg standard coal	20.17
Water wall and roof superheater	1612.94	kJ/kg standard coal	9.03
Platen superheater	294.24	kJ/kg standard coal	1.65
High temperature superheater	151.55	kJ/kg standard coal	0.85
High temperature reheater	164.36	kJ/kg standard coal	0.92
Low temperature reheater	451.35	kJ/kg standard coal	2.53
Low temperature superheater	307.81	kJ/kg standard coal	1.72
Economizer	244.12	kJ/kg standard coal	1.37
Air preheater	376.01	kJ/kg standard coal	2.10

Table 10. Distribution of heat transfer exergy loss of boiler under 50% BMCR load.

Parameter	Notation	Unit	Percentage of Fuel Exergy (%)
Total	3438.39	kJ/kg standard coal	19.25
Water wall and roof superheater	1915.10	kJ/kg standard coal	10.72
Platen superheater	259.71	kJ/kg standard coal	1.45
High temperature superheater	119.96	kJ/kg standard coal	0.67
High temperature reheater	109.73	kJ/kg standard coal	0.62
Low temperature reheater	275.58	kJ/kg standard coal	1.54
Low temperature superheater	208.91	kJ/kg standard coal	1.17
Economizer	220.74	kJ/kg standard coal	1.24
Air preheater	328.66	kJ/kg standard coal	1.84

**Figure 8.** Boiler overall exergy efficiency changes with load.

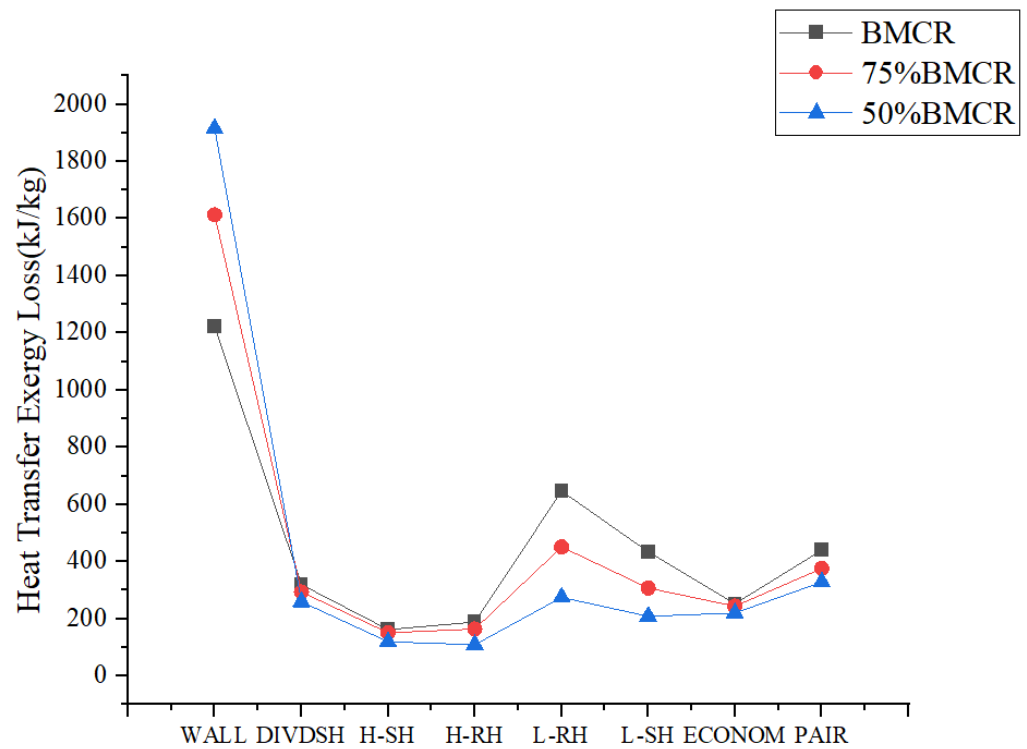


Figure 9. Variation of heat transfer exergy loss under different loads.

5. Comparison between Improved Scheme and Original Scheme

The boiler system is improved by increasing the heat transfer area of the air preheater and decreasing the heat transfer area of the economizer. The economizer and air preheater are located in one of the dual tail flues in the original scheme. In addition to changing the heat transfer area, the economizer is placed behind the flue to enhance the heat transfer effect of the air preheater. This reduces the heat absorption of the flue gas of the economizer, and the waste heat is given to the air preheater. Thus, the furnace heat transfer temperature difference and the combustion exergy loss are reduced. The improved process is shown in Figure 10. Blue lines indicate water vapor routes, while red lines indicate smoke routes.

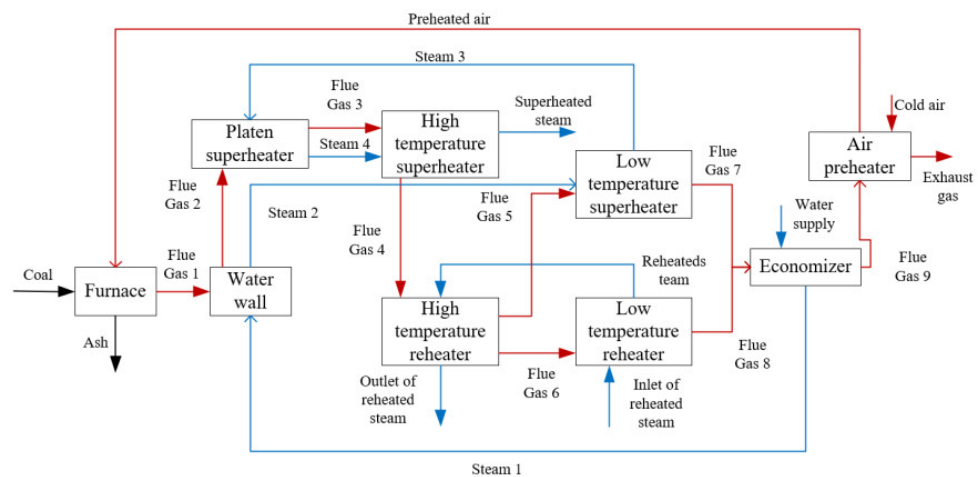


Figure 10. Flow chart of improved system.

In addition, this caused the working fluid temperature in the economizer to decrease as well. The amount of fuel should be adjusted accordingly, resulting in changes in the main steam and reheat steam temperatures. The input parameters of the model after transformation are shown in Table 11.

Table 11. Model parameters of improved scheme.

Environment	Temperature 25 °C. Pressure 10,325 Pa
Air	Under BMCR condition, oxygen 289,686 kg/h, nitrogen 1,089,769 kg/h
To-water	Temperature 284.7 °C, pressure 28.87 MPa, flow 1,110,000 kg/h
Main steam	Temperature 576 °C, pressure 25.40 MPa, flow 1,110,000 kg/h
Reheat steam inlet	Temperature 323 °C, pressure 4.524 MPa, flow 929,170 kg/h
Reheat steam outlet	Temperature 574 °C, pressure 4.334 MPa
Amount of fuel	184,070 kg/h

Figure 11 shows the comparison between the improved and the original heat transfer exergy loss distributions. A change in economizer location and structure resulted in a decrease in economizer exergy loss while an increase in air preheater exergy loss. In addition, the furnace must be adjusted to compensate for the low working fluid temperature at the exit of the economizer. The arrangement of the double flues at the rear was changed, resulting in a reduction in the heat transfer exergy loss of the low-temperature superheater and the low-temperature reheater. Due to the higher temperature of the main steam and the reheated steam, the heat transfer exergy loss also increased. However, the total heat transfer exergy loss was less than initially estimated at 20.17%.

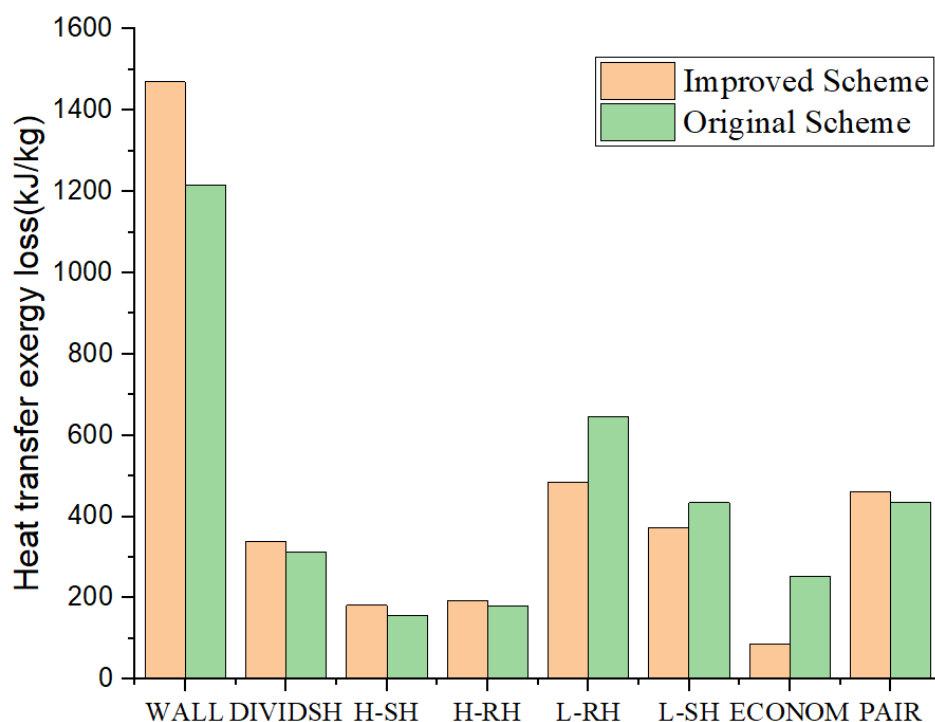
**Figure 11.** Comparison of heat transfer exergy loss distribution between the improved scheme and the original scheme.

Figure 12 shows a detailed comparison of exergy loss distributions between the improved and original schemes. Exergy efficiency is increased to 48.35%, and combustion exergy loss is significantly reduced. It is obvious that increasing the air preheating temperature has a significant impact on improving combustion and reducing the exergy loss of combustion, as well as slightly reducing the exergy loss of heat transfer. Due to the unchanged exhaust temperature, the external exergy loss remains the same. Thus, increasing the air preheat temperature and steam parameters will increase exergy efficiency. This paper provides a theoretical basis for the improvement plan of the power plant by adjusting the process and structure.

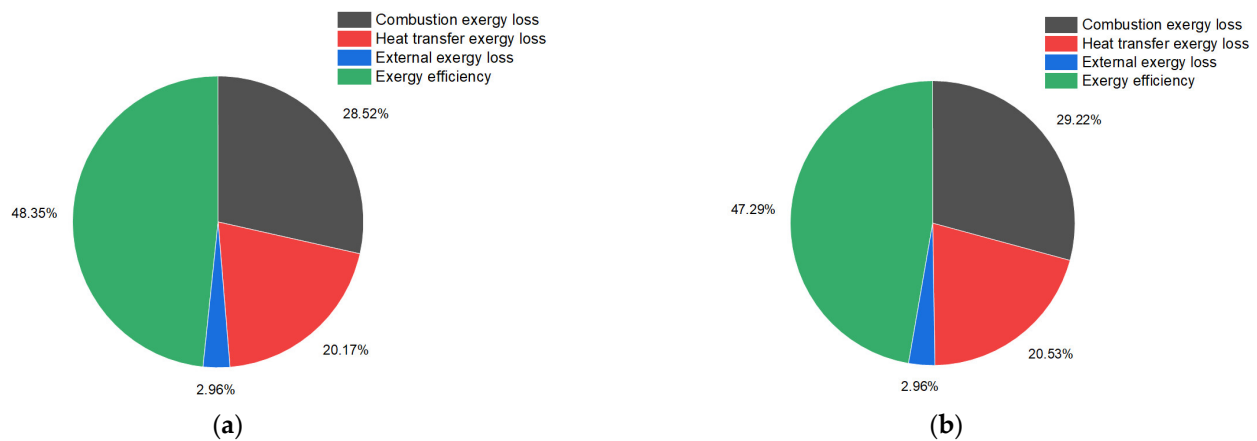


Figure 12. Comparison of exergy loss distribution between the improved scheme and the original scheme. (a) The exergy loss distribution of improved scheme. (b) The exergy loss distribution of original scheme.

6. Conclusions

In this paper, a one-dimensional model of a 350 MW power plant boiler was established by Aspen Plus. Based on the comparison between simulation results and operation data, the error in working fluid is within 5%, and the error in flue gas value is within 9%, proving the accuracy and feasibility of the one-dimensional model. Then, the efficiency of the boiler is maximized by changing the internal structure. The conclusions are as follows:

(1) The power plant boiler has an exergy efficiency of approximately 50%. Among the exergy losses, combustion exergy losses account for the most significant proportion, accounting for approximately 30%. In addition to the heat transfer exergy loss, approximately 20% of the energy is lost through external exergy losses. The exergy efficiency of the power station boiler also decreases as the load decreases, and the overall exergy loss gradually rises. Therefore, avoiding low-load operation can improve energy efficiency.

(2) The calculation and comparison of heat transfer exergy losses are carried out for each superheater and reheater in the rear flue. Due to the significant heat transfer temperature difference and exergy loss value, the heat transfer exergy loss value of the water wall and low-temperature reheater are relatively large.

(3) An improved scheme is proposed in this paper, which plays a role in reducing the heat exchange capacity of the economizer and increasing the heat exchange capacity of the air preheater. The combustion temperature of the boiler is increased, and the combustion exergy loss of the boiler is reduced. By improving the steam parameters, the exergy loss of heat transfer is reduced, and the exergy efficiency of the boiler is improved.

(4) The simulation results indicate a 48.35% increase in boiler exergy efficiency when the boiler's preheated air temperature and steam parameters are increased. The exergy loss of combustion is significantly reduced, as is the exergy loss of heat transfer. Results of the improvement plan show that the aim of improving exergy efficiency and saving energy was achieved, as well as providing a theoretical basis for improving the power plant.

Author Contributions: Conceptualization, W.L.; Writing—original draft, H.Y.; Writing—review & editing, Y.J. and L.L. All authors have read and agreed to the published version of the manuscript.

Funding: The authors would like to acknowledge the financial support of the Royal Academy of Engineering of the United Kingdom under the Newton Fund—the UK–China Industry Academia Partnership scheme (UK-CIAPP\201).

Conflicts of Interest: The authors declare no conflict of interest.

Nomenclature

		Unit
BMCR	Boiler Maximum Continuous Rating	
COLD-AIR	Cold Air	
DIVIDSH	Divider Superheater	
ECON	Economizer	
ECONOM	Economizer	
H-RH	High-Temperature Reheater	
H-SH	High-Temperature Superheater	
HOT-AIR	Hot Air	
IN-RH	Reheated Steam	
L-RH	Low-Temperature Reheater	
L-SH	Low-Temperature Superheater	
PHAIR	Air Preheater	
SOFA	Separate over Fire Air	
TOPH	Roof Superheater	
WALL	Water Cooled Wall	
a_B	Fuel Exergy Calculation	kJ/mol
a_2	Boiler External Loss	kJ/mol
A_{ar}	Received base ash	%
A_c	Heat Transfer Exergy Loss	kJ/mol
$A_{x,g}$	Income Exergy	kJ/mol
$A_{x,L}$	Exergy Loss	kJ/mol
$A_{x,n}$	Total Input Exergy.	kJ/mol
A^y	Applied Base Ash	%
c_{lz}	Specific Heat of Slag	kJ/kg
c_{lz}^c	Content of Slag	%
c_{fh}^c	Content of Fly Ash	%
c_{fh}	Specific Heat of Fly Ash	kJ/kg
c_p	Average Constant Pressure Specific Heat of Flue Gas	kJ/kg
C_{ar}	Received base carbon	%
C_p	Average Constant Pressure Specific Heat of Flue Gas	kJ/(m ³ ·K)
H_{ar}	Received base hydrogen	%
I_r	Exergy Loss of Combustion	kJ/mol
M_{ar}	Received base moisture	%
M_{ad}	Air drying base moisture	%
M_f	Amount of Fuel	kg/h
N_{ar}	Received base nitrogen	%
O_{ar}	Received base oxygen	%
q_4	Heat Loss of Incomplete Combustion of Solid	%
q_3	Heat Loss of Incomplete combustion of Combustible Gas	%
δQ	Unit Heat Transfer	kJ/kg
$Q_{net.ar}$	lower heating value	kJ/kg
S_{ar}	Received base sulphur	%
t_{lz}	Slag Temperature Discharged from the Furnace	K
T_B	Average Temperature of the Working Fluid in the Heat Dissipation Part of the Boiler	K
$\overline{T_c}$	Average Temperature of the Cold Fluid	K
T_{c1}	Inlet Temperature of the Cold Fluid	K
T_{c2}	Outlet Temperature of the Cold Fluid	K
$\overline{T_h}$	Average Temperature of the Hot Fluid	K
T_{py}	Exhaust Temperature	K
T_0	Ambient Temperature	K
T_{h1}	Inlet Temperature of the Hot Fluid	K
T_{h2}	Outlet Temperature of the Hot Fluid	K
V_g	Volume of Flue Gas Produced Per Kilogram of Fuel	m ³ /kg
V_y	Flue Gas Volume	m ³ /kg
V_{daf}	Dry ash-free basis volatile	m ³ /kg

References

1. Lin, B.Q.; Omoju, O.E.; Okonkvvo, J.U. Factors influencing renewable electricity consumption in China. *Renew. Sustain. Energy Rev.* **2016**, *55*, 687–696. [[CrossRef](#)]
2. Wang, Q.; Chen, Y. Status and outlook of China's free-carbon electricity. *Renew. Sustain. Energy Rev.* **2010**, *14*, 1014–1025. [[CrossRef](#)]
3. Zhang, C.; Zhou, K.L.; Yang, S.L.; Shao, Z. On electricity consumption and economic growth in China. *Renew. Sustain. Energy Rev.* **2017**, *76*, 353–368. [[CrossRef](#)]
4. Hu, Y.A.; Cheng, H.F. Development and Bottlenecks of Renewable Electricity Generation in China: A Critical Review. *Environ. Sci. Technol.* **2013**, *47*, 3044–3056. [[CrossRef](#)] [[PubMed](#)]
5. Bhattacharyya, S.C. Thermal Power-Generation and Environment—A Review of the Indian Case. *Int. J. Energy Res.* **1995**, *19*, 185–198. [[CrossRef](#)]
6. Nakatani, Y.; Wakamatsu, K.; Shindo, T.; Ito, Y. The Status of Thermoelectric Generation System. *IEEE Trans. Electr. Electron. Eng.* **2009**, *4*, 4–5. [[CrossRef](#)]
7. Li, Z.X.; Wang, D.D.; Lv, D.W.; Li, Y.; Liu, H.Y.; Wang, P.L.; Liu, Y.; Liu, J.Q.; Li, D.D. The geologic settings of Chinese coal deposits. *Int. Geol. Rev.* **2018**, *60*, 548–578. [[CrossRef](#)]
8. Wang, Q.; Li, R.R. Journey to burning half of global coal: Trajectory and drivers of China's coal use. *Renew. Sustain. Energy Rev.* **2016**, *58*, 341–346. [[CrossRef](#)]
9. Zhang, H.N.; Zhang, X.P.; Yuan, J.H. Coal power in China: A multi-level perspective review. *Wiley Interdiscip. Rev. Energy Environ.* **2020**, *9*, e386. [[CrossRef](#)]
10. Lv, T.; Guo, Z.W.; Gao, Y.; IEEE. Power Plant Boiler Waste Heat Recycling Design Research. In Proceedings of the 2012 Asia-Pacific Power and Energy Engineering Conference (APPEEC), Shanghai, China, 27–29 March 2012.
11. Lv, T.; Liu, L.Y.; Kun, L. Research on Testing of Burning Lignite in 1000MW Ultra Supercritical Concurrent Boiler. In *Advanced Materials Research*; Trans Tech Publications Ltd.: Bäch, Switzerland, 2012; Volume 347, pp. 3736–3739.
12. Seyedan, B.; Dhar, P.L.; Gaur, R.R.; Bindra, G.S. Optimization of waste heat recovery boiler of a combined cycle power plant. *J. Eng. Gas Turbines Power Trans. ASME* **1996**, *118*, 561–564. [[CrossRef](#)]
13. Wang, J.J.; Zhao, Z.N.; Xu, L.W.; Yao, W.Y. Scheme Analysis of Capacity-increasing Transformation for Reheaters of 300MW Boilers in a Power Plant. In Proceedings of the 2013 International Conference on Materials for Renewable Energy and Environment (ICMREE), Nanjing, China, 15–16 May 2013; IEEE: Piscataway, NJ, USA, 2013; Volume 1–3, pp. 698–702.
14. Wang, J.S.; Zhong, J.L.; Gou, X.L. Control strategy study on frequency and peak-load regulation of coal-fired power plant based on boiler heat storage capacity. *Proc. Inst. Mech. Eng. Part A J. Power Energy* **2018**, *232*, 1063–1078. [[CrossRef](#)]
15. Dincer, I.; Rosen, M.A. *Exergy and Energy Analyses*; Elsevier: Amsterdam, The Netherlands, 2013; pp. 21–30.
16. Kotas, T.J.; Mayhew, Y.R.; Raichura, R.C. Nomenclature for Exergy Analysis. *Proc. Inst. Mech. Eng. Part A J. Power Energy* **1995**, *209*, 275–280. [[CrossRef](#)]
17. Wall, G. Exergy tools. *Proc. Inst. Mech. Eng. Part A J. Power Energy* **2003**, *217*, 125–136. [[CrossRef](#)]
18. Eboh, F.C.; Ahlstrom, P.; Richards, T. Exergy Analysis of Solid Fuel-Fired Heat and Power Plants: A Review. *Energies* **2017**, *10*, 165. [[CrossRef](#)]
19. Liu, J.; Wang, Y.B.; He, C.B.; Zhu, P. Fuzzy Comprehensive Evaluation on Energy-efficiency of Plant Boiler based on Exergy Analysis. In *Advanced Materials Research*; Trans Tech Publications Ltd.: Bäch, Switzerland, 2014; pp. 1022–1026.
20. Mahfuz, M.H.; Kamyar, A.; Afshar, O.; Sarraf, M.; Anisur, M.R.; Kibria, M.A.; Saidur, R.; Metselaar, I. Exergetic analysis of a solar thermal power system with PCM storage. *Energy Convers. Manag.* **2014**, *78*, 486–492. [[CrossRef](#)]
21. Tontu, M.; Bilgili, M.; Sahin, B. Performance analysis of an industrial steam power plant with varying loads. *Int. J. Exergy* **2018**, *27*, 231–250. [[CrossRef](#)]
22. Zhu, S.H.; Zhang, M.; Huang, Y.Q.; Wu, Y.X.; Yang, H.R.; Lyu, J.F.; Gao, X.Y.; Wang, F.J.; Yue, G.X. Thermodynamic analysis of a 660 MW ultra-supercritical CFB boiler unit. *Energy* **2019**, *173*, 352–363. [[CrossRef](#)]
23. Behbahania, A.; Ramezani, S.; Hejrandoost, M.L. A loss method for exergy auditing of steam boilers. *Energy* **2017**, *140*, 253–260. [[CrossRef](#)]
24. Rangel-Hernandez, V.H.; Damian-Ascencio, C.; Belman-Flores, J.M.; Zaleta-Aguilar, A. Assessing the Exergy Costs of a 332-MW Pulverized Coal-Fired Boiler. *Entropy* **2016**, *18*, 300. [[CrossRef](#)]
25. Saidur, R.; Ahamed, J.U.; Masjuki, H.H. Energy, exergy and economic analysis of industrial boilers. *Energy Policy* **2010**, *38*, 2188–2197. [[CrossRef](#)]
26. Terhan, M.; Comakli, K. Energy and exergy analyses of natural gas-fired boilers in a district heating system. *Appl. Therm. Eng.* **2017**, *121*, 380–387. [[CrossRef](#)]
27. Yang, D.; Xu, H.; Chen, H.P.; Jia, R.X. Analysis of the Exergy Efficiency and Influencing Factor of CFB Boiler. In Proceedings of the ICEET: 2009 International Conference on Energy and Environment Technology, Guilin, China, 16–18 October 2009; IEEE: Piscataway, NJ, USA, 2009; Volume 1, pp. 522–525.
28. Shi, Y.H.; Li, Q.; Wen, J.; Cui, F.S.; Pang, X.Q.; Jia, J.F.; Zeng, J.C.; Wang, J.C. Soot Blowing Optimization for Frequency in Economizers to Improve Boiler Performance in Coal-Fired Power Plant. *Energies* **2019**, *12*, 2901. [[CrossRef](#)]

-
29. Gomez, M.A.; Martin, R.; Collazo, J.; Porteiro, J. CFD Steady Model Applied to a Biomass Boiler Operating in Air Enrichment Conditions. *Energies* **2018**, *11*, 2513. [[CrossRef](#)]
 30. Feng, J.; Shen, Y. *Boiler Principle and Calculation*; Science Press: Beijing, China, 1998; Volume 787.